

Slippage on which interface in nanopore filtration?

Xiaoxu Huang¹, Wei Li¹ and Yongbin Zhang^{*2}

¹School of Mechanical Technology, Wuxi Institute of Technology, Gaolang Xilu 1600, 214121, Wuxi, Jiangsu Province, China

²College of Mechanical Engineering, Changzhou University, Gehu Lu 21, Wujin, 213164, Changzhou, Jiangsu Province, China

(Received August 11, 2023, Revised April 1, 2024, Accepted April 2, 2024)

Abstract. The flow in a nanopore of filtration membrane is often multiscale and consists of both the adsorbed layer flow and the intermediate continuum fluid flow. There is a controversy on which interface the slippage should occur in the nanopore filtration: On the adsorbed layer-pore wall interface or on the adsorbed layer-continuum fluid interface? What is the difference between these two slippage effects? We address these subjects in the present study by using the multiscale flow equations incorporating the slippage on different interfaces. Based on the limiting shear strength model for the slippage, it was found from the calculation results that for the hydrophobic pore wall the slippage surely occurs on the adsorbed layer-pore wall interface, however for the hydrophilic pore wall, the slippage can occur on either of the two interfaces, dependent on the competition between the interfacial shear strength on the adsorbed layer-pore wall interface and that on the adsorbed layer-continuum fluid interface. Since the slippage on the adsorbed layer-pore wall interface can be designed while that on the adsorbed layer-continuum fluid interface can not, the former slippage can result in the flux through the nanopore much higher than the latter slippage by designing a highly hydrophobic pore wall surface. The obtained results are of significant interest to the design and application of the interfacial slippage in nanoporous filtration membranes for both improving the flux and conserving the energy cost.

Keywords: adsorbed layer; fluid; mass transport; multiscale; nanopore; slippage

1. Introduction

Nanoporous filtration membranes have been evolved lately especially in manufacturing because of its application value in ultra filtration (Ariono *et al.* 2018, Baker and Bird 2008, Bottino *et al.* 2011, Brown *et al.* 1975, El-ghzizel *et al.* 2019, Elizabeth *et al.* 2012, Fissel *et al.* 2009, Jackson and Hillmyer 2010, Jin *et al.* 2019, Sanjay *et al.* 2021, Sofos 2021, Stavrogiannis *et al.* 2022, Surwade *et al.* 2015). There have been plentiful experimental researches on the fluid flow in nanopores (Grüener *et al.* 2016, Harrell *et al.* 2006, Holt *et al.* 2006, Huang *et al.* 2015, Itoh *et al.* 2022, Koklu *et al.* 2017, Majumder *et al.* 2005, Nair *et al.* 2012, Radha *et al.* 2016, Secchi *et al.* 2016, Wu *et al.* 2019). Molecular dynamics simulation (MDS) can be regarded as a computer experiment and it was often used in the modeling of fluid flow in nanopores (Ho *et al.* 2011, Jiang and Zhang 2022, Kannam *et al.* 2013, Wagemann *et al.* 2019, Walther *et al.* 2013, Wang *et al.* 2012).

Some particular phenomena were found by MDS in nanopore flows such as the rheology evolution, the fluid slippage and the sticking layer (Calabrò *et al.* 2013, Liu and Li 2011, Mattia and Calabro 2012, Meyer *et al.* 1998, Myers 2011, Shaat 2017, Sofos *et al.* 2015, Thomas and McGaughey 2008, 2009). However, such flows are not yet fully understood.

One of the most obvious facts is the existence of the molecule layers physically adsorbed to the solid nanopore

wall (Brown *et al.* 1975, Grosse-Rhode and Findenegg 1978, Koklu *et al.* 2017, Liu and Li 2011, Sofos *et al.* 2015). When the diameter of the nanopore is critically small, there is only the adsorbed layer inside the nanopore, and the nanopore flow is thus essentially non-continuum (Zhang 2006, 2016). However, when the nanopore size is not very small so that both the adsorbed layer flow and the intermediate continuum fluid flow occur inside the pore, the nanopore flow is actually multiscale and it is also the popular flow mode in nanoporous filtration membrane (Adiga *et al.* 2009, Jiang *et al.* 2020, Wang and Zhang 2022). Inside the hydrophilic silica nanopore, it was found that the water flow rate can be very significantly reduced due to the formation of the sticking boundary layer on the pore wall (Koklu *et al.* 2017). However, inside the hydrophobic nanopore such as the carbon nanotube, the water flow rate was found to be several orders higher than that calculated from the Hagen-Poiseuille equation (Holt *et al.* 2006, Majumder *et al.* 2005, Mattia and Calabro 2012, Whitby and Quirke 2007). This unexpected phenomenon was attributed to the interfacial slippage (Holt *et al.* 2006, Majumder *et al.* 2005, Mattia and Calabro 2012, Whitby and Quirke 2007). In the hydrophilic nanopore flow, the interfacial slippage was also detected (Tran-Duc *et al.* 2019). Nevertheless, it is not very clear whether the slippage occurs on the adsorbed layer-pore wall interface or on the adsorbed layer-continuum fluid interface. According to the limiting shear strength model (Zhang 2014), when the pore wall is hydrophobic so that the shear strength of the adsorbed layer-pore wall interface is far lower than that of the adsorbed layer-continuum fluid interface, the slippage should occur on the adsorbed layer-pore wall interface;

*Corresponding author, Professor,
E-mail: engmech1@sina.com

however for the hydrophilic pore wall, due to the entropy discontinuity, it was regarded that the shear strength of the adsorbed layer-continuum fluid interface would be remarkably lower than that of the adsorbed layer-pore wall interface, and the slippage would occur on the adsorbed layer-continuum fluid interface (Rozeanu and Tipei 1980), nevertheless this was only a physical speculation and lacked quantitative analysis. Currently, it is still not very sure that where the slippage occurs in a real nanopore flow and on which interface the slippage will be most beneficial to the flux of a nanoporous membrane.

In this paper, from the multiscale flow analysis, we quantitatively explore on which interface the slippage occurs in the nanopore flow in nanoporous filtration membranes, by calculating the critical power losses on the nanopore respectively for the slippage occurring on the adsorbed layer-pore wall interface and on the adsorbed layer-continuum fluid interface. Then, the total volume flow rates through the nanopore are compared when the slippage occurs respectively on these two interfaces. The advantage of the slippage on which interface is thus clearly shown. The present study is theoretically fresh and important for us to understand in detail the slippage mechanism in the nanopore filtration (e.g. the slippage does not necessarily occur on the adsorbed layer-continuum fluid interface but may instead occur on the adsorbed layer-pore wall interface in a hydrophilic nanopore). It can guide the design of the best slippage for efficiently improving the flux through the nanoporous membrane.

2. Multiscale flow in the nanopore

When the nanopore is not so small that both the adsorbed molecule layers and the continuum fluid coexist inside the pore, the nanopore flow should generally be treated as the multiscale flow although the adsorbed layer might be solidified. Fig. 1 shows the circumstance inside this nanopore. There may be several molecule layers in the adsorbed layer which can be equivalently treated as Fig. 1 shows, due to the fluid-pore wall interaction. The adsorbed layer flow is non-continuum, influenced by the evolution of the rheological property within the layer and the slippage occurring on the adsorbed layer-pore wall interface or on the adsorbed layer-continuum fluid interface. When the pore radius ($R_0 + h_{bf}$) is about one hundred times larger than the thickness (h_{bf}) of the adsorbed layer, the adsorbed layer flow is negligible and the flow in the whole pore can be treated as continuum (Lin *et al.* 2022). When $1 < (R_0 + h_{bf})/h_{bf} < 100$, the adsorbed layer flow should generally be considered, and it would considerably contribute to the total flow rate through the nanopore.

3. Multiscale analysis

Classical multiscale approaches model the adsorbed layer flow by full molecular dynamics simulation and model the intermediate continuum fluid flow by the continuum fluid model (Atkas and Aluru 2002, Yen *et al.*

2007). This approach is difficult to apply for the pore in Fig. 1 where its dimensions are impractical to simulate, since it would demand high computational time and memory. For solving this problem, Zhang has derived the closed-form explicit flow equations respectively for the adsorbed layer flow and the intermediate continuum fluid flow in the nanopore in Fig. 1 when the interfacial slippage is respectively absent, occurs on the adsorbed layer-pore wall interface, or occurs on the adsorbed layer-continuum fluid interface, by equivalently treating the adsorbed layer as Fig. 1 shows. In the present study, we just borrow his analytical results.

The interfacial slippage was interpreted as the result of the interfacial shear stress exceeding the interfacial shear strength (Zhang 2014). This limiting shear strength model for the interfacial slippage is different from the slip length model (Gennes de 2002, Vinogradova 1995), where the slip length is actually a fictitious parameter (Zhang 2014). The limiting shear strength model is believed to be physically more rational and applicable for much wider engineering cases than the constant slip length model (Zhang 2014). In some circumstances they are reconciled, but in most engineering flows the slip length is not constant and the interfacial limiting shear strength model is much more accurate than the constant slip length model (Zhang 2014).

The present study uses the interfacial limiting shear strength model to characterize the interfacial slippage. According to this model, the shear stress on the interface is expressed as:

$$\tau = \begin{cases} \eta\gamma, & \text{for } |\tau| < \tau_s \\ \text{sign}(\gamma)\tau_s, & \text{for } |\tau| \geq \tau_s \end{cases} \quad (1)$$

where τ_s is the shear strength of the interface, that is the maximum endurable shear stress of the interface, and η and γ are respectively the effective viscosity and the shear strain rate of the fluid on the interface. Eq. (1) interprets that when the magnitude of the interfacial shear stress (τ) is smaller than the interfacial shear strength (τ_s), the velocity boundary condition should be applied, the flow velocity on the interface should follow the continuity condition, and the fluid shear stress on the interface should be calculated according to the fluid rheological behavior; however, it interprets that when the magnitude of τ is greater than that of τ_s , the shear stress boundary condition should be applied on the interface, and the magnitude of the fluid shear stress on the interface should be equal to the interfacial shear strength. When the shear stress boundary condition is applied on the interface, the velocity on the interface is not continuous, and the velocity difference on the interface is the interfacial slipping velocity. This well explains the interfacial slippage from both physics and mathematics. For more understanding, people can refer to the reference by Zhang (2014), where the interfacial slipping velocities have been derived for some specific engineering flow problems based on the interfacial limiting shear strength model.

The present interfacial slippage model physically follows the observation that the interfacial slippage more easily occurs on the hydrophobic surface than on the hydrophilic surface due to the weak and strong fluid-solid surface interactions on these surfaces respectively. The

following assumptions are also used: (a) The intermediate continuum fluid is Newtonian; (b) The pressure across the pore radius is constant; (c) The influences of the fluid pressure on the fluid density and viscosity are negligible; (d) The flow is isothermal.

3.1 Critical power loss on the pore for starting the interfacial slippage

The dimensionless critical power loss on the whole pore (with the axial length l) in Fig. 1 for starting the slippage which occurs on the adsorbed layer-pore wall interface is:

$$K_{cr,bf-w} = \left[\frac{1}{2\lambda_{bf} \left(1 + \frac{D(n-1)}{R_0}\right)} \right]^2 \left\{ 2\pi \frac{R_e}{R_0} \left\{ \frac{4\varepsilon\lambda_{bf}^3}{C_y \left(1 + \frac{\Delta x}{D}\right)} \left[1 + \frac{1}{2\lambda_{bf}} - \frac{\Delta_{n-2}(q_0 - q_0^n)}{h_{bf}(q_0^{n-1} - q_0^n)} \right] - \frac{2F_1\lambda_{bf}^3}{3C_y} \right\} + \frac{\pi}{4} - \frac{4\pi}{C_y} \left\{ \frac{F_2\lambda_{bf}^2}{6} - \frac{\lambda_{bf}}{1 + \frac{\Delta x}{D}} \left[\frac{1}{2} + \lambda_{bf} - \frac{\Delta_{n-2}(q_0 - q_0^n)}{2R_0(q_0^{n-1} - q_0^n)} \right] \right\} \right\} \quad (2)$$

where $K_{cr,bf-w} = POW_{cr,bf-w}\eta/(\tau_{s,bf-w}^2 h_{bf}^2 l)$, $POW_{cr,bf-w}$ is the dimensional critical power loss on the whole pore for starting the slippage, η is the fluid bulk viscosity, l is the axial length of the pore, $\tau_{s,bf-w}$ is the shear strength of the interface between the adsorbed layer and the pore wall, h_{bf} is the thickness of the adsorbed layer, $\lambda_{bf} = h_{bf}/(2R_0)$, R_0 is the radius of the circle covered by the continuum fluid as shown in Fig. 1, D is the fluid molecule diameter, n is the equivalent number of the fluid molecules across the adsorbed layer thickness, R_e is the equivalent constant radius and often $R_e/R_0 = 1 + \lambda_{bf}$, Δx is the separation between the neighboring fluid molecules in the circumferential direction in the adsorbed layer, $C_y = \eta_{bf}^{eff}/\eta$, η_{bf}^{eff} is the effective viscosity of the adsorbed layer, $q_0 (>1)$ is the average value of Δ_{j+1}/Δ_j (Δ_j is the separation between the $(j+1)^{th}$ and j^{th} fluid molecules across the adsorbed layer thickness), $POW_{cr,bf-f}$ is the separation between the neighboring fluid molecules across the adsorbed layer thickness just on the boundary between the adsorbed layer and the intermediate continuum fluid,

$$F_1 = \frac{\eta_{bf}^{eff}}{h_{bf}^3} (12D^2\Psi + 6D\Phi) \quad (3)$$

$$\varepsilon = \frac{2DI + II}{h_{bf}(n-1)(\Delta_l/\eta_{line,l})_{avr,n-1}} \quad (4)$$

$$F_2 = \frac{6\eta_{bf}^{eff} D(n-1)}{h_{bf}^2} (\Delta_{l-1}/\eta_{line,l-1})_{avr,n-1} \quad (5)$$

ε is the parameter reflecting the non-continuum effect of the adsorbed layer on the Couette flow of the adsorbed layer, F_1 is the parameter reflecting the non-continuum effect of the adsorbed layer on the Poiseuille flow of the adsorbed layer, and F_2 is the parameter reflecting the non-

continuum effect of the adsorbed layer on the Poiseuille flow of the intermediate continuum fluid (Zhang 2020). Here,

$$I = \sum_{i=1}^{n-1} i(\Delta_l/\eta_{line,l})_{avr,i} \quad (6)$$

$$\Psi = \sum_{i=1}^{n-1} i(\Delta_{l-1}/\eta_{line,l-1})_{avr,i} \quad (7)$$

$$II = \sum_{i=0}^{n-2} \left[i(\Delta_l/\eta_{line,l})_{avr,i} + (i+1)(\Delta_l/\eta_{line,l})_{avr,i+1} \right] \Delta_i \quad (8)$$

$$\Phi = \sum_{i=0}^{n-2} \left[i(\Delta_{l-1}/\eta_{line,l-1})_{avr,i} + (i+1)(\Delta_{l-1}/\eta_{line,l-1})_{avr,i+1} \right] \Delta_i \quad (9)$$

$$i(\Delta_l/\eta_{line,l})_{avr,i} = \sum_{j=1}^i \Delta_{j-1}/\eta_{line,j-1} \quad (10)$$

$$i(\Delta_{l-1}/\eta_{line,l-1})_{avr,i} = \sum_{j=1}^i j\Delta_{j-1}/\eta_{line,j-1} \quad (11)$$

$\eta_{line,j-1}$ is the local viscosity between the j^{th} and $(j-1)^{th}$ fluid molecules across the adsorbed layer thickness.

When the dimensional power loss on the whole pore (with the axial length l) is no more than $POW_{cr,bf-w}$, no wall slippage occurs; otherwise, the wall slippage occurs and it can result in the total flow rate through the pore far higher than that calculated from the classical Hagen-Poiseuille equation. In carbon nanotubes or in biological systems, due to the hydrophobic pore wall and the low values of $\tau_{s,bf-w}$, the values of $POW_{cr,bf-w}$ are low, and just a very small power loss on the nanochannel causes the severe wall slippage and consequently the high water flux through the channel, not explainable from the classical hydrodynamic flow theory (Holt *et al.* 2006, Majumder *et al.* 2005, Mattia and Calabro 2012, Whitby and Quirke 2007).

The dimensionless critical power loss on the whole nanopore (with the axial length l) in Fig. 1 for starting the slippage which occurs on the adsorbed layer-continuum fluid interface is:

$$K_{cr,bf-f} = \frac{1}{4\lambda_{bf}^2} \left\{ 8\pi \frac{R_e}{R_0} \left\{ \frac{\varepsilon\lambda_{bf}^3}{C_y \left(1 + \frac{\Delta x}{D}\right)} \left[1 + \frac{1}{2\lambda_{bf}} - \frac{\Delta_{n-2}(q_0 - q_0^n)}{h_{bf}(q_0^{n-1} - q_0^n)} \right] - \frac{F_1\lambda_{bf}^3}{6C_y} \right\} + \frac{\pi}{4} - \frac{4\pi}{C_y} \left\{ \frac{F_2\lambda_{bf}^2}{6} - \frac{\lambda_{bf}}{1 + \frac{\Delta x}{D}} \left[\frac{1}{2} + \lambda_{bf} - \frac{\Delta_{n-2}(q_0 - q_0^n)}{2R_0(q_0^{n-1} - q_0^n)} \right] \right\} \right\} \quad (12)$$

where $K_{cr,bf-f} = POW_{cr,bf-f}\eta/(\tau_{s,bf-f}^2 h_{bf}^2 l)$, $POW_{cr,bf-f}$ is the dimensional critical power loss on the whole nanopore for starting the slippage, $\tau_{s,bf-f}$ is the shear strength of the interface between the adsorbed layer and the continuum fluid, and the other parameters are same as above.

Table 1 The mean specific growth rate and maximum growth rate of *Anabaena*

Interaction	Parameter		
	a ₀	a ₁	a ₂
Strong	1.8335	-1.4252	0.5917
Medium	1.0822	-0.1758	0.0936
Weak	0.9507	0.0492	1.6447E-4

For a given nanopore, if $POW_{cr,bf-w} < POW_{cr,bf-f}$, the slippage first occurs on the adsorbed layer-pore wall interface and it is absent on the adsorbed layer-continuum fluid interface; otherwise, the slippage only occurs on the adsorbed layer-continuum fluid interface. The competition between these two parameter values depends on the difference between $\tau_{s,bf-w}$ and $\tau_{s,bf-f}$ and also the difference between the calculated values of $K_{cr,bf-w}$ and $K_{cr,bf-f}$.

3.2 Total volume flow rates through the nanopore for different interfacial conditions

For no slippage occurrence, the dimensionless total volume flow rate through the nanopore is:

$$Q_v = \frac{(\pi K_1)^2}{4\lambda_{bf}^2} \left\{ 8 \frac{R_e}{R_0} \frac{\varepsilon \lambda_{bf}^3}{C_y \left(1 + \frac{\Delta x}{D}\right)} \left[1 + \frac{1}{2\lambda_{bf}} - \frac{\Delta_{n-2}(q_0 - q_0^n)}{h_{bf}(q_0^{n-1} - q_0^n)}\right] - \frac{4R_e F_1 \lambda_{bf}^3}{3R_0 C_y} + \frac{1}{4} - \frac{4}{C_y} \left\{ \frac{F_2 \lambda_{bf}^2}{6} - \frac{\lambda_{bf}}{1 + \frac{\Delta x}{D}} \left[\frac{1}{2} + \lambda_{bf} - \frac{\Delta_{n-2}(q_0 - q_0^n)}{2R_0(q_0^{n-1} - q_0^n)} \right] \right\} \right\}^{1/2} \quad (13)$$

where $Q_v = q_v \eta / (\tau_s h_{bf}^3)$, q_v is the dimensional total volume flow rate through the nanopore, τ_s is $\tau_{s,bf-w}$ or $\tau_{s,bf-f}$, K_1 is the dimensionless power loss on the whole nanopore and $K_1 = POW \eta / (\tau_s^2 h_{bf}^2 l)$, POW is the dimensional power loss on the whole nanopore.

When the slippage only occurs on the adsorbed layer-pore wall interface, the dimensionless total volume flow rate through the nanopore is:

$$Q_{v,bf-w} = K_1 \left[1 + \frac{1}{2\lambda_{bf}} - \frac{1 + \frac{\Delta_{n-2}(q_0 - q_0^n)}{D(q_0^{n-1} - q_0^n)}}{2\lambda_{bf} \frac{R_0}{D}} \right], \quad (14)$$

for $K_1 > K_{cr,bf-w}$

where $Q_{v,bf-w} = q_v \eta / (\tau_{s,bf-w} h_{bf}^3)$.

When the slippage only occurs on the adsorbed layer-continuum fluid interface, the dimensionless total volume flow rate through the nanopore is:

$$Q_{v,bf-f} = \frac{K_1}{2\lambda_{bf}}, \text{ for } K_1 > K_{cr,bf-f} \quad (15)$$

where $Q_{v,bf-f} = q_v \eta / (\tau_{s,bf-f} h_{bf}^3)$.

The comparison between the values of $Q_{v,bf-w}$ and $Q_{v,bf-f}$ can show the slippage on which interface is better for yielding the higher flux of the nanopore.

4. Calculation

The calculations chose: $\Delta x/D = \Delta_{n-2}/D = 0.15$

These parameter values are representative for the simple fluid flows in silicon or carbon nanopores like those of water and methane (Jiang and Zhang 2022 and 2024, Zhang 2016). It was assumed that $\eta_{line,i}/\eta_{line,i+1} = q_0^m$, where m is positive constant (Jiang and Zhang 2022).

The following regressed equations were used (Zhang 2020):

$$\varepsilon = (4.56E - 6) \left(\frac{\Delta_{n-2}}{D} + 31.419 \right) (n + 133.8) (q_0 + 0.188)(m + 41.62) \quad (16)$$

$$F_1 = 0.18 \left(\frac{\Delta_{n-2}}{D} - 1.905 \right) (\ln n - 7.897) \quad (17)$$

$$F_2 = (-3.707E - 4) \left(\frac{\Delta_{n-2}}{D} - 1.99 \right) (n + 64) (q_0 + 0.19)(m + 42.43) \quad (18)$$

$$Cy(H_{bf}) = a_0 + \frac{a_1}{H_{bf}} + \frac{a_2}{H_{bf}^2} \quad (19)$$

where $H_{bf} = h_{bf}/h_{cr,bf}$, $h_{cr,bf}$ is the critical thickness for characterizing the rheological properties of the adsorbed layer, and a_0 , a_1 and a_2 are respectively constant. The accuracies of Eqs. (16)-(18) are satisfactory as compared to the direct calculations (Zhang 2020). Eq. (19) also fits the experimental measurements (Meyer *et al.* 1998, Zhang 2004).

For different fluid-pore wall interactions, the following parameter values were used:

Weak interaction: $m = 0.5, n = 3, q_0 = 1.03, h_{cr,bf} = 7\text{nm}$

Medium interaction: $m = 1.0, n = 5, q_0 = 1.1, h_{cr,bf} = 20\text{nm}$

Strong interaction: $m = 1.5, n = 8, q_0 = 1.2, h_{cr,bf} = 40\text{nm}$

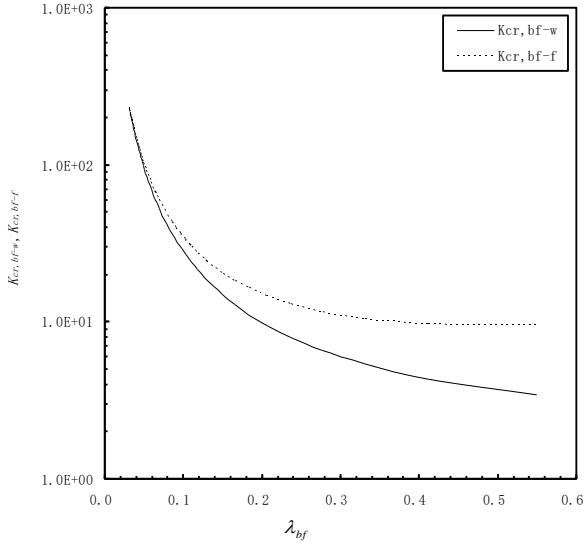
These parameter values surely give different discontinuity and inhomogeneity across the adsorbed layer thickness owing to different fluid-pore wall interaction strengths for the flow of simple fluids in nanopores (Zhang 2015a, b, 2016).

The other parameter values are shown in Table 1. These parameter values result in different effective viscosities of the adsorbed layer due to different fluid-pore wall interactions according to Eq. (19). Stronger the fluid-pore wall interaction, more significant the solidification of the adsorbed layer, and greater the value of Cy . The parameter values in Table 1 fit the experimental measurements of the viscosity of simple fluids confined in nanochannels (Meyer *et al.* 1998, Zhang 2004).

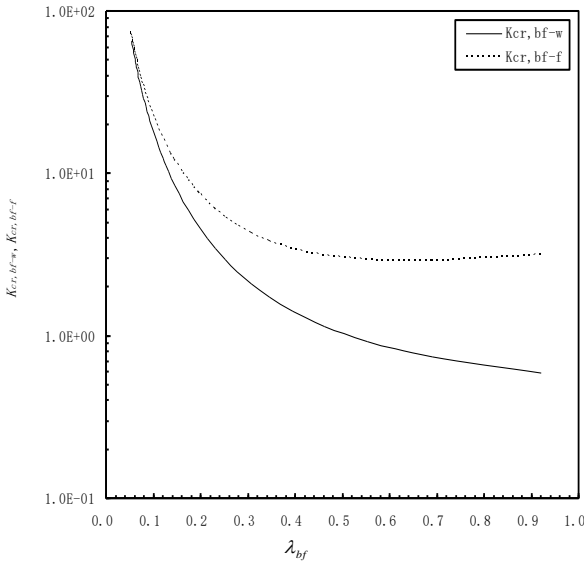
5. Results

5.1 Critical power loss on the pore for starting the slippage

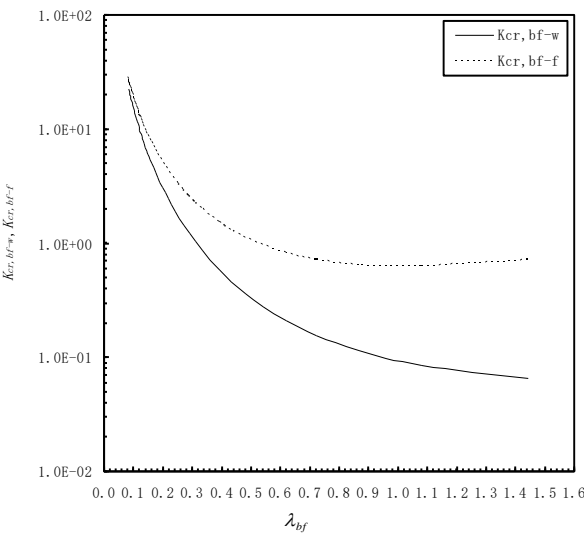
Fig. 2(a) shows that for the weak fluid-pore wall interaction, the value of $K_{cr,bf-w}$ is smaller than that of



(a) For the weak interaction



(b) For the medium interaction



(c) For the strong interaction

Fig. 2 Values of $K_{cr,bf-w}$ and $K_{cr,bf-f}$ for different fluid-pore wall interactions

$K_{cr,bf-f}$ for a given λ_{bf} ; the difference between $K_{cr,bf-w}$ and $K_{cr,bf-f}$ is increased with the increase of λ_{bf} , and it is very significant for $\lambda_{bf} \geq 0.1$ and is great for $\lambda_{bf} \geq 0.4$. According to the definitions of $K_{cr,bf-w}$ and $K_{cr,bf-f}$, for the strongly hydrophobic nanopore wall (which yields the quite weak fluid-pore wall interaction), the dimensional critical power loss $POW_{cr,bf-w}$ on the nanopore for starting the slippage on the adsorbed layer-pore wall interface should be significantly smaller than the dimensional critical power loss $POW_{cr,bf-f}$ on the nanopore for starting the slippage on the adsorbed layer-continuum fluid interface since $\tau_{s,bf-w}$ is significantly smaller than $\tau_{s,bf-f}$. This means that for the strongly hydrophobic nanopore wall, the slippage occurs on the adsorbed layer-pore wall interface and its occurrence is much easier than the occurrence of the slippage on the adsorbed layer-continuum fluid interface for $\lambda_{bf} \geq 0.1$. It is particularly the case for a larger λ_{bf} i.e. a smaller nanopore.

Fig. 2(b) shows the similar results of $K_{cr,bf-w}$ and $K_{cr,bf-f}$ for the medium fluid-pore wall interaction as in Fig. 2(a). The medium interaction should reflect the pore wall which is somewhat hydrophilic. From Fig. 2(b), it seems hard to judge on which interface the slippage should occur. As an example, for $\lambda_{bf} = 0.9$, $K_{cr,bf-f}/K_{cr,bf-w} = 5.444$; for this case, if $\tau_{s,bf-w} < 2.333\tau_{s,bf-f}$, $POW_{cr,bf-w} < POW_{cr,bf-f}$ and the slippage thus occurs on the adsorbed layer-pore wall interface, otherwise the slippage should occur on the adsorbed layer-continuum fluid interface. It was found that the slippage can also occur in a hydrophilic nanopore (Tran-Duc *et al.* 2019). According to the present results, this slippage can occur either on the adsorbed layer-pore wall interface or on the adsorbed layer-continuum fluid interface, depending on the competition between $\tau_{s,bf-w}$ and $\tau_{s,bf-f}$.

Fig. 2(c) shows the similar results of $K_{cr,bf-w}$ and $K_{cr,bf-f}$ for the strong fluid-pore wall interaction as in Figs. 2(a)-(b). The strong interaction should correspond to the strongly hydrophilic nanopore wall for which the shear strength ($\tau_{s,bf-w}$) of the adsorbed layer-pore wall interface is much higher than that ($\tau_{s,bf-f}$) of the adsorbed layer-continuum fluid interface. In a strongly hydrophilic nanopore, there is a sticking boundary layer and the slippage occurs more difficultly (Koklu *et al.* 2017). Figure 2(c) shows that for $\lambda_{bf}=1.4$, $K_{cr,bf-f}/K_{cr,bf-w} \approx 10$; for this case, if $\tau_{s,bf-w} > 3.162\tau_{s,bf-f}$, $POW_{cr,bf-w} > POW_{cr,bf-f}$ and the slippage thus only occurs on the adsorbed layer-continuum fluid interface. In a strongly hydrophilic nanopore, such a condition is often satisfied. However, in this nanopore, to generate the slippage on the adsorbed layer-continuum fluid interface is much more difficult than to generate the slippage on the adsorbed layer-pore wall interface in a hydrophobic nanopore, due to $\tau_{s,bf-w} \ll \tau_{s,bf-f}$. This is why the hydrophobic nanopore wall is far advantageous over the strongly hydrophilic nanopore wall by the resulting wall slippage to largely increase the nanopore transport. Such a technical merit can be easily realized just by covering a hydrophobic coating on the nanopore wall.

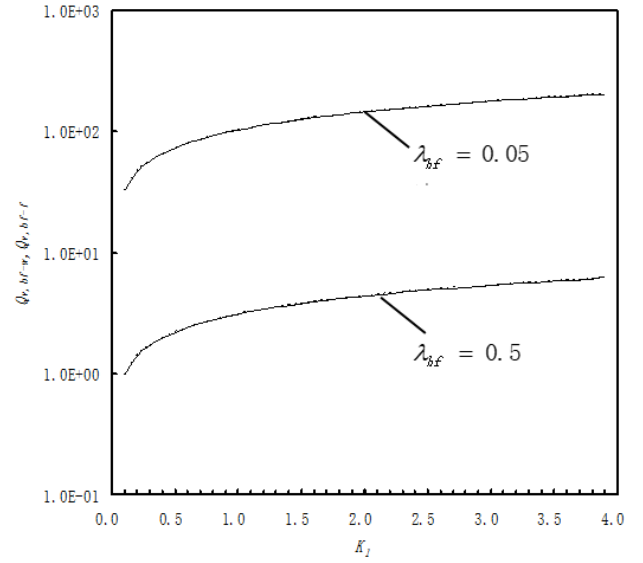
5.2 Nanopore transport for the slippage on different interfaces

Fig. 3(a) shows the comparison of the values of $Q_{v,bf-w}$ and $Q_{v,bf-f}$ for the weak fluid-pore wall interaction for the dimensionless power loss K_1 on the whole pore covering the ranges of no slippage and slippage. Generally, even for a weak fluid-pore wall interaction, the slippage does not necessarily occur on the adsorbed layer-pore wall interface, and it can also occur on the adsorbed layer-continuum fluid interface depending on the competition between $\tau_{s,bf-w}$ and $\tau_{s,bf-f}$; thus for the purpose of comparison the value of $Q_{v,bf-f}$ here is also calculated for the weak fluid-pore wall interaction. When no slippage occurs, $Q_{v,bf-w}$ or $Q_{v,bf-f}$ are calculated from Eq. (3). Fig. 3(a) shows that for the two λ_{bf} values the curves for $Q_{v,bf-w}$ and $Q_{v,bf-f}$ are overlaid. This means that for the weak interaction, if $\tau_{s,bf-w} = \tau_{s,bf-f}$, the same dimensional power loss (*POW*) on the pore (giving the same dimensionless power loss K_1 on the pore) gives nearly the same volume flow rate through the pore whenever the slippage occurs on the adsorbed layer-pore wall interface or on the adsorbed layer-continuum fluid interface. However, since the adsorbed layer-pore wall interface can be modified by the coating and the value of $\tau_{s,bf-w}$ and the slippage on this interface can thus be designed, we prefer the slippage to occur on the adsorbed layer-pore wall interface to enhance the nanopore transport by using the hydrophobic pore wall.

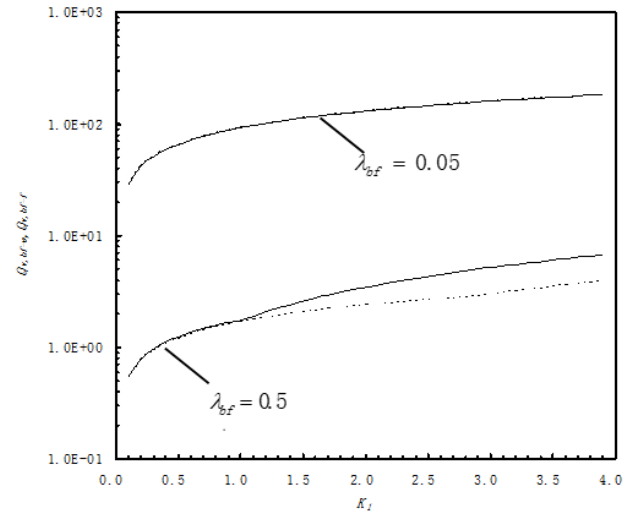
Fig. 3(b) shows that for the medium fluid-pore wall interaction, for $\lambda_{bf} = 0.05$ the curves for $Q_{v,bf-w}$ and $Q_{v,bf-f}$ are overlaid. This is due to the negligible adsorbed layer effect because of the pore radius far larger than the thickness of the adsorbed layer. It means that for this case, if $\tau_{s,bf-w} = \tau_{s,bf-f}$, the nanopore transport is not influenced by the interface where the slippage occurs. As the medium interaction corresponds to the hydrophilic pore wall which gives $\tau_{s,bf-w} > \tau_{s,bf-f}$, for very low λ_{bf} values the slippage should be better to occur on the adsorbed layer-continuum fluid interface to give higher flow rate through the pore for the medium interaction.

Fig. 3(b) shows that for $\lambda_{bf} = 0.5$, the curves for $Q_{v,bf-w}$ and $Q_{v,bf-f}$ are overlaid when K_1 is below about 1.0. This corresponds to the case of no slippage on any interface. However, when K_1 is above about 1.0, for a given λ_{bf} the value of $Q_{v,bf-w}$ is larger than that of $Q_{v,bf-f}$ due to the slippage occurrence on the two interfaces. This means that for the medium interaction, when the radius of the nanopore is comparable to the thickness of the adsorbed layer, the slippage on the adsorbed layer-pore wall interface should generate a more flow rate through the pore than the slippage on the adsorbed layer-continuum fluid interface if $\tau_{s,bf-w}$ is only modestly larger than $\tau_{s,bf-f}$.

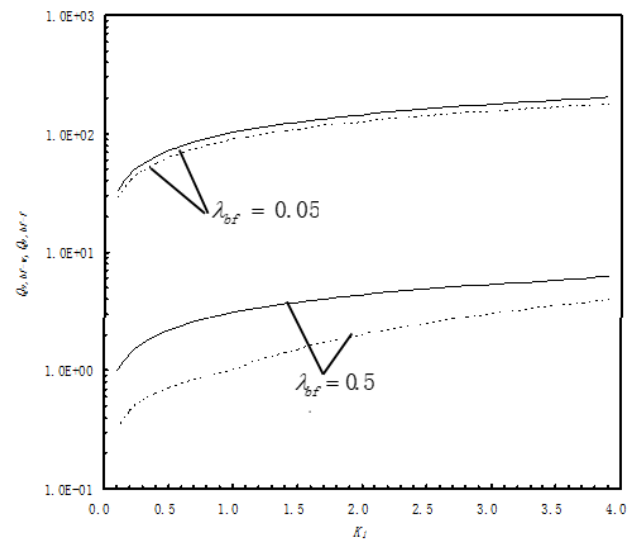
Fig. 3(c) compares the total volume flow rates ($Q_{v,bf-w}$ and $Q_{v,bf-f}$) through the pore when the pore wall is respectively hydrophobic and strongly hydrophilic (so that the slippage respectively occurs on the adsorbed layer-pore wall interface and on the adsorbed layer-continuum fluid interface). Even for $\lambda_{bf} = 0.05$, the slippage for hydro-



(a) For the weak interaction



(b) For the medium interaction



(c) Solid line: hydrophobic pore wall, dashed line: strongly hydrophilic pore wall

Fig. 3 Comparison of the values of $Q_{v,bf-w}$ (solid line) and $Q_{v,bf-f}$ (dashed line)

phobic pore wall gives the flow rate through the pore significantly higher than that given by the slippage for strongly hydrophilic pore wall when $\tau_{s,bf-w} = \tau_{s,bf-f}$ and the dimensional power losses on the pore for the two cases are the same. In practice, the value of $\tau_{s,bf-w}$ for a hydrophobic pore wall is remarkably smaller than that of $\tau_{s,bf-f}$, thus even when λ_{bf} is very low so that the pore radius is far bigger than h_{bf} the nanopore transport for a hydrophobic pore wall should be much higher than that for a strongly hydrophilic pore wall.

When $\lambda_{bf} = 0.5$ so that the pore radius is comparable to the thickness of the adsorbed layer, Fig. 3(c) shows that the value of $Q_{v,bf-w}$ for a hydrophobic pore wall is far larger than that of $Q_{v,bf-f}$ for a strongly hydrophilic pore wall in the condition of the slippage respectively occurring on the two interfaces when the values of K_1 are the same. This indicates that in a small nanopore the hydrophobic pore wall very effectively enhances the mass transport. It suggests the strong benefit of the application of a hydrophobic pore wall in a very small nanopore.

6. Validation of the model

By comparing full molecular dynamics simulation results with the results calculated from Zhang's multiscale approach as shown in this paper, Jiang and Zhang (2024) showed the correctness and accuracy of the present multiscale scheme in calculating the total volume flow rate through a nanochannel. Currently are absent the results in other literatures showing the dependences of the total flow rate through a nanopore on the power loss and on the interfacial shear strength in the case of the wall slippage. The direct comparison of the present results with the results from other sources is still not viable. The present study should be the first step and for correlation by the following researches.

7. Conclusions

Multiscale calculations were held to show where the slippage should occur in the nanopore where both the adsorbed layer flow and the intermediate continuum fluid flow occur. This multiscale flow nanopore is applicable to nanoporous filtration membranes, biological nanochannel flows, and nanopore mass transfer etc. The study on this subject is important for the application of the slippage for efficiently improving the mass transfer through the nanopore.

The closed-form explicit flow equations for the nanopore multiscale flow derived by Zhang were used to calculate the critical power losses on the whole pore for starting the slippage respectively on the adsorbed layer-pore wall interface and on the adsorbed layer-continuum fluid interface. For these two slippage cases, the volume flow rates through the nanopore were also respectively calculated.

According to the calculation results, we conclude that:

- when the nanopore wall is hydrophobic, the slippage

should occur on the adsorbed layer-pore wall interface, and this interfacial slippage can greatly enhance the nanopore transport with low interfacial shear strengths especially for a very small nanopore.

- For a medium-hydrophilic nanopore, the slippage can occur on the adsorbed layer-pore wall interface or on the adsorbed layer-continuum fluid interface, depending on the competition between the shear strength ($\tau_{s,bf-w}$) of the adsorbed layer-pore wall interface and the shear strength ($\tau_{s,bf-f}$) of the adsorbed layer-continuum fluid interface ($\tau_{s,bf-w} > \tau_{s,bf-f}$); if $\tau_{s,bf-w}$ is close to $\tau_{s,bf-f}$, the slippage occurs on the adsorbed layer-pore wall interface especially for a very small nanopore; if the difference between $\tau_{s,bf-w}$ and $\tau_{s,bf-f}$ is sufficiently large, the slippage occurs on the adsorbed layer-continuum fluid interface.

- When the nanopore is medium-hydrophilic, for very low λ_{bf} values i.e. big nanopores the slippage should be better to occur on the adsorbed layer-continuum fluid interface for giving higher flow rate through the pore; when the radius of the nanopore is comparable to the thickness of the adsorbed layer, the slippage on the adsorbed layer-pore wall interface should generate a more flow rate through the pore than the slippage on the adsorbed layer-continuum fluid interface if $\tau_{s,bf-w}$ is only modestly larger than $\tau_{s,bf-f}$.

- When the nanopore is strongly hydrophilic, the slippage should occur on the adsorbed layer-continuum fluid interface due to $\tau_{s,bf-w}$ much higher than $\tau_{s,bf-f}$.

References

- Adiga, S.P., Jin, C., Curtiss, L.A., Monteiro-Riviere, N.A. and Narayan, R. J. (2009), "Nanoporous membranes for medical and biological applications", *Nanomed. Nanobiotech.*, **1**(5), 568-581. <https://doi.org/10.1002/wnan.50>.
- Ariono, D., Aryanti, P.T.P., Wardani, A.K. and Wenten, I.G. (2018), "Fouling characteristics of humic substances on tight polysulfone-based ultrafiltration membrane", *Membr. Water Treat.*, **9**(5), 353-361. <https://doi.org/10.12989/mwt.2018.9.5.353>.
- Atkas, O. and Aluru, N.R. (2002), "A combined continuum/DSMC technique for multiscale analysis of microfluidic filters", *J. Comput. Phys.*, **178**(2), 342-372. <https://doi.org/10.1006/jcph.2002.7030>.
- Baker, L.A. and Bird, S.P. (2008), "Nanopores: A makeover for membranes", *Nature Nanotech.*, **3**, 73-74. <https://doi.org/10.1038/nnano.2008.13>.
- Bottino, A., Capannelli, G., Comite, A., Ferrari, F. and Firpo, R. (2011), "Water purification from pesticides by spiral wound nanofiltration membrane", *Membr. Water Treat.*, **2**(1), 63-74. <http://doi.org/10.12989/mwt.2011.2.1.063>.
- Brown, C.E., Everett, D.H., Powell, A.V. and Thome, P.E. (1975), "Adsorption and structuring phenomena at the solid/liquid interface", *Faraday Discus. Chem. Soc.*, **59**, 97-108. <https://doi.org/10.1039/DC9755900097>.
- Cadotte, J.E., Petersen, R.J., Larson, R.E. and Erickson, E.E. (1980), "A new thin film composite seawater reverse osmosis membrane", *Desali.*, **32**(1), 25-31. [https://doi.org/10.1016/S0011-9164\(00\)86003-8](https://doi.org/10.1016/S0011-9164(00)86003-8).
- Calabrò, F., Lee, K.P. and Mattia, D. (2013), "Modelling flow enhancement in nanochannels: Viscosity and slippage", *Appl.*

- Math. Lett.*, **26**(10), 991-994.
<https://doi.org/10.1016/j.aml.2013.05.004>.
- Cohen-Tanugi, D., Lin, L.C. and Grossman, J.C. (2016), "Multi-layer nanoporous graphene membranes for water desalination", *Nano Lett.*, **16**(2), 1027.
<https://doi.org/10.1021/acs.nanolett.5b04089>.
- Oliveira, E.E.M., Barbosa, C.C.R. and Afonso, J.C. (2012), "Selectivity and structural integrity of a nanofiltration membrane for treatment of liquid waste containing uranium", *Membr. Water Treat.*, **3**(4), 231-242.
<http://doi.org/10.12989/mwt.2012.3.4.231>.
- El-ghezizel, S., Jalté, H., Zeggar, H., Zait, M., Belhamidi, S., Tiyal, F., Hafsi, M., Taky, M. and Elmidaoui, A. (2019), "Autopsy of nanofiltration membrane of a decentralized demineralization plant", *Membr. Water Treat.*, **10**(4), 277-286.
<https://doi.org/10.12989/mwt.2019.10.4.277>.
- Fissel, W.H., Dubnisheva, A., Eldridge, A.N., Fleischman, A.J., Zydney, A.L. and Roy, S. (2009), "High-performance silicon nanopore hemofiltration membranes", *J. Membr. Sci.*, **326**(1), 58-63. <http://doi.org/10.1016/j.memsci.2008.09.039>.
- Gennes de, P.G. (2002), "On fluid/wall slippage", *Langmuir*, **18**, 3413-3414. <https://doi.org/10.1021/la0116342>
- Grosse-Rhode, M. and Findenegg, G.H. (1978), "Formation of ordered monolayers of *n*-alkanes at the cleavage face of nickel chloride", *J. Coll. Interf. Sci.*, **64**(2), 374-376.
[https://doi.org/10.1016/0021-9797\(78\)90375-2](https://doi.org/10.1016/0021-9797(78)90375-2).
- Gruener, S., Wallacher, D., Greulich, S., Busch, M. and Huber, P. (2016), "Hydraulic transport across hydrophilic and hydrophobic nanopores: Flow experiments with water and *n*-hexane", *Phys. Rev. E*, **93**(1), 013102.
<https://doi.org/10.1103/PhysRevE.93.013102>.
- Harrell, C.C., Siwy, Z.S. and Martin, C.R. (2006), "Conical nanopore membranes: Controlling the nanopore shape", *Small*, **2**(2), 157. <https://doi.org/10.1002/sml.200690004>.
- Ho, T.A., Papavassiliou, D.V., Lee, L.L. and Striolo, A. (2011), "Liquid water can slip on a hydrophilic surface", *PNAS*, **108**(39), 16170-16175. <https://doi.org/10.1073/pnas.110518910>.
- Holt, J.K., Park, H.G., Wang, Y., Staermandn, M., Artyukhin, A.B., Grigoropoulos, C.P., Noy, A. and Bakajin, O. (2006), "Fast mass transport through sub-2-nanometer carbon nanotubes", *Science*, **312**(5776), 1034-1037.
<https://doi.org/10.1126/science.1126298>.
- Huang, L., Zhang, M., Li, C. and Shi, G. (2015), "Graphene-based membranes for molecular separation", *J. Phys. Chem. Lett.*, **6**(14), 2806-2815. <https://doi.org/10.1021/acs.jpcclett.5b00914>.
- Itoh, Y., Chen, S., Hirahara, R., Konda, T., Aoki, T., Ueda, T., Shimada, I., Cannon, J.J., Shao, C., Shiomi, J., Tabata, K.V., Noji, H., Sato, K. and Aida, T. (2022), "Ultrafast water permeation through nanochannels with a densely fluorinated interior surface", *Science*, **376**(6594), 738-743.
<https://doi.org/10.1126/science.abd0966>.
- Jackson, E.A. and Hillmyer, M.A. (2010), "Nanoporous membranes derived from block copolymers: From drug delivery to water filtration", *ACS Nano*, **4**(7), 3548-3553.
<http://doi.org/10.1021/nn1014006>.
- Jiang, C.T. and Zhang, Y.B. (2022), "Direct matching between the flow factor approach model and molecular dynamics simulation for nanochannel flows", *Sci. Rep.*, **12**, 396.
<https://doi.org/10.1038/s41598-021-04391-5>.
- Jiang, C.T. and Zhang, Y.B. (2024), "Comparisons between full molecular dynamics simulation and Zhang's multiscale scheme for nanochannel flows", *J. Mol. Mod.*, In Press.
- Jiang, X.B., Shao, Y., Li, J., Wu, M., Niu, Y., Ruan, X., Yan, X., Li, X. and He, G. (2020), "Bioinspired hybrid micro/nano-structure composited membrane with intensified mass transfer and antifouling for high saline water membrane distillation", *ACS Nano*, **14**(12), 17376-17386.
<https://doi.org/10.1021/acs.nano.0c07543>.
- Jin, Y., Choi, Y., Song, K.G., Kim, S. and Park, C. (2019), "Iron and manganese removal in direct anoxic nanofiltration for indirect potable reuse", *Membr. Water Treat.*, **10**(4), 299-305.
<https://doi.org/10.12989/mwt.2019.10.4.299>.
- Kannam, S.K., Todd, B.D., Hansen, J.S. and Daivis, P.J. (2013), "How fast does water flow in carbon nanotubes?", *J. Chem. Phys.*, **138**, 094701. <http://doi.org/10.1063/1.4793396>.
- Koklu, A., Li, J., Sengor, S. and Beskok, A. (2017), "Pressure-driven water flow through hydrophilic alumina nanomembranes", *Microfluid. Nanofluid.*, **21**, 124.
<https://doi.org/10.1007/s10404-017-1960-1>.
- Lin, W., Li, J. and Zhang, Y.B. (2022), "Mass transfer in the filtration membrane covering from macroscale, multiscale to nanoscale", *Membr. Water Treat.*, **13**(4), 167-172.
<https://doi.org/10.12989/mwt.2022.13.4.167>.
- Liu, C. and Li, Z. (2011), "On the validity of the Navier-Stokes equations for nanoscale liquid flows: The role of channel size", *AIP Adv.*, **1**(3), 032108. <https://doi.org/10.1063/1.3621858>.
- Majumder, M., Chopra, N., Andrews, R. and Hinds, B.J. (2005), "Enhanced flow in carbon nanotubes", *Nature*, **438**, 44.
<https://doi.org/10.1038/438044a>.
- Mattia, D. and Calabro, F. (2012), "Explaining high flow rate of water in carbon nanotubes via solid-liquid molecular interactions", *Microfluid. Nanofluid.*, **13**, 125-130.
<https://doi.org/10.1007/s10404-012-0949-z>.
- Meyer, E., Overney, R.M., Dransfeld, K. and Gyalog, T. (1998), *Friction and Rheology on the Nanometer Scale*, World Scientific Press, New Jersey, NJ, USA.
- Myers, T.G. (2011), "Why are slip lengths so large in carbon nanotubes?" *Microfluid. Nanofluid.*, **10**, 1141-1145.
<https://doi.org/10.1007/s10404-010-0752-7>.
- Nair, R.R., Wu, H.A., Jayaram, P.N., Grigorieva, I.V. and Geim, A.K. (2012), "Unimpeded permeation of water through helium-leak-tight graphene based membranes", *Science*, **335**(6067), 442-444. <https://doi.org/10.1126/science.1211694>.
- Radhal, A., Esfandiari, F., Wang, A.P., Rooney, K., Gopinadhan, A., Keerthi, A., Mishchenko, A., Janardanan, P., Fumagalli, M., Lozada-Hidalgo, S., Garaj, S.J., Haigh, I.V., Grigorieva, H.A. and Wu, A.K. (2016), "Molecular transport through capillaries made with atomic-scale precision", *Nature*, **538**, 222-225.
<https://doi.org/10.1038/nature19363>.
- Rozeanu, L. and Tipei, N. (1980), "Slippage phenomena at the interface between the adsorbed layer and the bulk of the lubricant: Theory and experiment", *Wear*, **64**(2), 245-257.
[https://doi.org/10.1016/0043-1648\(80\)90131-3](https://doi.org/10.1016/0043-1648(80)90131-3).
- Sanjay, R., Nagarajan, P., Sabyasachi, G., Subhadip, M., Suryasarathi, B. and Narayan, Ch.D. (2021), "Porous graphene-based membranes: Preparation and properties of a unique two-dimensional nanomaterial membrane for water purification", *Separ. Purif. Rev.*, **50**(3), 262-282.
<https://doi.org/10.1080/15422119.2020.1725048>.
- Secchi, E., Marbach, S., Niguès, A., Siria, A. and Bocquet, L. (2016), "Massive radius-dependent flow slippage in carbon nanotubes", *Nature*, **537**, 210-213.
<https://doi.org/10.1038/nature19315>.
- Shaht, M. (2017), "Viscosity of water interfaces with hydrophobic nanopores: Application to water flow in carbon nanotubes", *Langmuir*, **33**(44), 12814-12819.
<https://doi.org/10.1021/acs.langmuir.7b02752>.
- Sofos, F. (2021), "A water/ion separation device: theoretical and numerical investigation", *Appl. Sci.*, **11**(18), 8548.
<https://doi.org/10.3390/app11188548>.
- Sofos, F., Karakasidis, T.E. and Liakopoulos, A. (2015), "Fluid structure and system dynamics in nanodevices for water desalination", *Desali. Water Treat.*, **57**(25), 11561-11571.
<https://doi.org/10.1080/19443994.2015.1049966>.

- Stavrogiannis, C., Sofos, F., Karakasidis, T.E. and Vavougiou, D. (2022), "Investigation of water desalination/purification with molecular dynamics and machine learning techniques", *AIMS Mater. Sci.*, **9**(6), 919-938. <https://doi.org/10.3934/matserci.2022054>.
- Surwade, S.P., Smirnov, S.N., Vlasiouk, I.V., Unocic, R.R., Veith, G.M., Dai, S. and Mahurin, S.M. (2015), "Water desalination using nanoporous single-layer graphene", *Nature Nanotech.*, **10**, 459-464. <https://doi.org/10.1038/nnano.2015.37>.
- Thomas, J.A. and McGaughey, A.J.H. (2008), "Density, distribution, and orientation of water molecules inside and outside carbon nanotubes", *J. Chem. Phys.*, **128**(8), 084715. <https://doi.org/10.1063/1.2837297>.
- Thomas, J.A. and McGaughey, A.J.H. (2009), "Water flow in carbon nanotubes: Transition to subcontinuum transport", *Phys. Rev. Lett.*, **102**(18), 184502. <https://doi.org/10.1103/PhysRevLett.102.184502>.
- Tran-Duc, T., Phan-Thien, N. and Wang, J. (2019), "A theoretical study of permeability enhancement for ultrafiltration ceramic membranes with conical pores and slippage", *Phys. Fluids*, **31**(2), 022003. <https://doi.org/10.1063/1.5085140>.
- Vinogradova, O.I. (1995), "Drainage of a thin liquid film confined between hydrophobic surfaces", *Langmuir*, **11**, 2213-2220. <https://doi.org/10.1021/la00006a059>
- Wagemann, E., Walther, J.H., Cruz-Chu, E.R. and Zambrano, H.A. (2019), "Water flow in silica nanopores coated by carbon nanotubes from a wetting translucency perspective", *J. Phys. Chem.*, **123**(42), 25635-25642. <https://doi.org/10.1021/acs.jpcc.9b05294>.
- Walther, J.H., Ritos, K., Cruz-Chu, E.R., Megaridis, C.M. and Koumoutsakos, P. (2013), "Barriers to superfast water transport in carbon nanotube membranes", *Nano Lett.*, **13**(5), 1910-1914. <https://doi.org/10.1021/nl304000k>.
- Wang, L., Dumont, R. and Dickson, J.M. (2012), "Nonequilibrium molecular dynamics simulation of water transport through carbon nanotube membranes at low pressure", *J. Chem. Phys.*, **137**(4), 044102. <https://doi.org/10.1063/1.4734484>.
- Wang, M. and Zhang, Y.B. (2022), "Water permeability through the wall of blood capillary", *Front. Heat Mass Transf.*, **18**, 7. <http://doi.org/10.5098/hmt.18.7>.
- Whitby, M. and Quirke, N. (2007), "Fluid flow in carbon nanotubes and nanopipes", *Nature Nanotech.*, **2**, 87-94. <https://doi.org/10.1038/nnano.2006.175>.
- Wu, K., Chen, Z., Li, J., Xu, J., Wang, K., Li, R., Wang, S. and Dong, X. (2019), "Ultra-high water flow enhancement by optimizing nanopore chemistry and geometry", *Langmuir*, **35**(26), 8867-8873. <https://doi.org/10.1021/acs.langmuir.9b01179>.
- Yen, T.H., Soong, C.Y. and Tzeng, P.Y. (2007), "Hybrid molecular dynamics-continuum simulation for nano/mesoscale channel flows", *Microfluid. Nanofluid.*, **3**, 665-675. <https://doi.org/10.1007/s10404-007-0154-7>.
- Zhang, Y.B. (2004), "Modeling of molecularly thin film elasto-hydrodynamic lubrication", *J. Balkan Trib. Assoc.*, **10**(3), 394-421.
- Zhang, Y.B. (2006), "Flow factor of non-continuum fluids in one-dimensional contact", *Industr. Lubri. Trib.*, **58**(3), 151-169. <https://doi.org/10.1108/00368790610661999>.
- Zhang, Y.B. (2014), "Review of hydrodynamic lubrication with interfacial slippage", *J. Balkan Trib. Assoc.*, **20**(4), 522-538.
- Zhang, Y.B. (2015a), "The flow factor approach model for the fluid flow in a nano channel", *Int. J. Heat Mass Transf.*, **89**, 733-742. <https://doi.org/10.1016/j.ijheatmasstransfer.2015.05.092>
- Zhang, Y.B. (2015b), "A quantitative comparison between the flow factor approach model and the molecular dynamics simulation results for the flow of a confined molecularly thin fluid film", *Theor. Comput. Fluid Dyn.*, **29**, 193-204. <https://doi.org/10.1007/s00162-015-0348-7>
- Zhang, Y.B. (2016), "The flow equation for a nanoscale fluid flow", *Int. J. Heat Mass Transf.*, **92**(1), 1004-1008. <https://doi.org/10.1016/j.ijheatmasstransfer.2015.09.008>.
- Zhang, Y.B. (2020), "Modeling of flow in a very small surface separation", *Appl. Math. Mod.*, **82**, 573-586. <https://doi.org/10.1016/j.apm.2020.01.069>.

CC